Effects of negativity bias on amygdala and anterior cingulate cortex activity in short and long emotional stimulation paradigms

視覚刺激提示条件の変化による否定性バイアスの影響について機能的MRIを用いた検討

吉田　宜清

鈴鹿医療科学大学大学院医療科学研究科医療科学専攻
博士（医療科学）の学位申請論文

指導教員　岡田　幸法　客員准教授

２０２２年３月

博　士　論　文　審　査　委　員

主査　安田　鋭介　教授

副査　柴田　幸一　教授

副査　荒井　信行　助教

DH19103 吉田　宜清

Effects of negativity bias on amygdala and anterior cingulate cortex activity in short and long emotional stimulation paradigms

医療科学専攻　　氏 名 吉田 宜清

(指導教員 ： 岡田 幸法 客員准教授)

【はじめに】 大うつ病性障害(major depression disorder: MDD)は、世界的に最も多い精神疾患の一つである。最近の functional MRI(fMRI)研究では扁桃体と前帯状皮質(anterior cingulate cortex: ACC)の機能障害が MDD の再現性のある優れたバイオマーカーであることが報告されている。扁桃体や ACC の活動量の変化を MDD のバイオマーカーとして用いる場合において、fMRI 検査での刺激パラダイムが短時間で単純なものであれば検査中の患者の不安や体動を軽減することができる。しかし、短く単純な刺激パラダイムを採用する場合、扁桃体や ACC の活性化がどのように影響するか考慮する必要がある。特に留意しなければならない点として、否定性バイアスがある。否定的バイアスは否定的な（不快な）刺激は同じように極端で刺激的な肯定的な（快い）刺激よりもより顕著な反応を引き起こす現象である。しかし、刺激パラダイムの長さと扁桃体や ACC の活性化との関係性について否定性バイアスの観点から検討した研究は現時点では存在していない。否定性バイアスはうつ病の脆弱性に関連する潜在的な認知特性である可能性があるため、短い刺激パラダイムにおける扁桃体の活性化に対する否定性バイアスの影響を調査することは非常に重要であると考えられる。

【目的】 感情と覚醒度の値が付けられている国際標準の情動写真集(international affective picture system: IAPS)を視覚刺激として用いfMRIの刺激パラダイム条件を変化させることにより、MDDの脆弱性に関連するといわれる否定性バイアスの観点より扁桃体とACCの感情関連脳領域に及ぼす影響を検討することである。

【方法】 1.被検者について 本研究は、東京大学医科学研究所にて倫理委員会で承認を受けた研究である(承認番号29-51-A1120)。説明を行い、同意を受けた27名（男性20名、女性7名、平均年齢22.4 ± 2.48歳、右利き）の被験者にて研究を行った。被検者についてはあらかじめ問診を行った。体内金属、心疾患、外傷、精神疾患歴を有する症例は認めなかった。被検者の体動が1 voxel(3.8 mm) 以上ないことを確認した。

2.タスクと手順 視覚刺激は申請を行いフロリダ大学から使用許可を得たIAPSから取得した写真を使用した。画像は快画像、不快画像、中立画像より構成した。1枚あたり提示時間は2秒間とした。選択したIAPSの快、不快、中立の画像の平均 valence/ arousal score は、快画像 7.1/ 7.3、中立画像 5.1/ 5.0、不快画像 3.0/ 2.9であった。視覚刺激はE-Primeソフトウェアを用いてプログラムした。本研究では、short-simple task（ST条件） とlong-complex task（LT条件） の2つのタスクを1セッションとした。ST条件は、5つのブロックを中立画像 30秒、不快画像 20秒、快画像 20秒に設定した。LT条件は、快画像、不快画像をそれぞれ30秒提示しその前後に中立画像をそれぞれ30秒提示した。また、参加者に映像が変わるごとに右手人差し指でボタンを押すよう求め、画像を知覚している (眠っていない) ことを確認した。快画像と不快画像の順序は被検者の半数ごとに変更した。

3.使用機器 MRI装置は、診療用3Tの装置を用いて撮像を行った(Siemens社製、skyra、ドイツ)。画像収集用のヘッドネックコイル20chを用い、尾側へスクリーンを配置し鏡を用いてスクリーンを視認できるようにした。EPI(echo planar imaging)シーケンスおよび3D T1強調グラディエントエコー法による解剖画像は、全脳を含めた撮像を行った。

4.画像解析 撮像したMRIデータの画像処理はSPM12を用いて、一般的なVBM(voxel based morphometry) 解析を行った。本研究では、中立画像を提示したときに収集されたデータをマスク画像と考え、快および不快画像データをマスク画像より差分して表示する4つのコントラスト画像を作成した。

5.Regions of interest (ROI)解析 ROI分析は、SPM(statistical parametric mapping)のtoolboxであるMarsBar-0.44を使用した。解剖学的ROIとして両側扁桃体とACCを使用し、それぞれのタスクおよび全タスクにおける快画像と不快画像から活動量の指標となる β 値を抽出した。否定性バイアスの影響を検討するため感情画像による活動

量を統計学的な解析(paired *t*-test)を行い、その効果量(Cohen's *d*)を算出した。統計解析ソフトはEZRを用いて有意水準はBonferroniで補正しそれぞれのタスクでは、$P < 0.025$、全タスクでは$P < 0.0125$として検定を行った。

【結果】 分析は、FDR(false discovery rate) corrected $p < 0.01$を用いて6個以上の連続voxelが賦活したものを用いた。不快画像を提示した場合、ST条件およびLT条件の両条件で扁桃体が活性化された。快画像の提示では、LT条件のみ扁桃体が活性化された。また、快・不快画像提示時のST条件およびLT条件で、ACCの不活性化が観察された(表1)。ACCは背側と腹側に区分され、背側ACCでは不快画像提示時のST条件およびLT条件にて不活性化が認められたが、腹側ACCでは、快画像を提示したST条件では、不活性化が認めなかった。扁桃体の抽出 β 値は、ST条件では不快画像と快画像を提示した時に有意な差を認め、その効果量は大きかった。その一方でLT条件では有意な差を認めたが、その効果量は小さかった。ACCは、ST条件で不快画像と快画像を提示した際の β 値の差を認めず、LT条件のみで差を認めたが、効果量は小さかった(表2)。

表1. 画像解析による解剖学的な活性化

		扁桃体	ACC
不快画像	ST	活性化を確認できる	抑制化を確認できる
	LT	活性化を確認できる	抑制化を確認できる
快画像	ST	活性化を確認できない	抑制化を確認できる
	LT	活性化を確認できる	抑制化を確認できる

表2. 解剖学的影響度の違い

	扁桃体	ACC
ST	影響が大きい	影響がない
LT	影響が少ない	影響が少ない

【考察】 画像解析の結果より、ST 条件では、不快画像が快画像よりも速く処理されることにより不快画像と快画像に対する扁桃体の活性化の違いを認めたと考えられる。ROI 解析の結果、ST 条件では 1 回目、2 回目、複合セッションでの扁桃体の抽出 β 値は、不快画像の方が快画像よりも有意に大きいことが示された。特に、効果量は大きく、ST 条件で最大値($d = 0.98$)を示した。これらの結果から、ST 条件は第 1 セッションから第 2 セッションにかけて否定性バイアスの影響を受けていることが示唆された。そのため不快画像では快適画像を提示した時に比べ偏桃体や ACC の活動が速かに処理された結果、ST 条件で不快画像の扁桃体の活性化が快適画像よりも大きかったと考えられる。一方、LT 条件での ROI 解析の結果、1 回目と 2 回目のセッションでは、不快画像と快画像の間で扁桃体の活動に差は見られなかった。複合セッションの β 値は、不快画像と快画像間で扁桃体活動に有意な差を示したが、LT 条件の効果量($d = 0.28$)は ST 条件($d = 0.98$)の場合よりも小さかった。これらの結果は、LT 条件では否定性バイアスの影響が小さくなっていることを意味していると考えられる。

ACC は ST 条件、LT 条件に関係なく不活性化を認めた。視覚刺激を用いた他の研究では ACC の活性化と不活性化の報告がある。これらの矛盾した報告は、ACC のサブ領域に起因している可能性がある。腹側 ACC は扁桃体との接続性が強いと報告されている。本研究では、扁桃体が活性化されていない場合には腹側 ACC の不活性化を認めなかった。その一方で、扁桃体が活性化しているときは腹側 ACC の不活性化を認めた。したがって、本研究で観察された腹側 ACC の不活性化は、扁桃体の過剰な活性化を防ぐためのコントローラーとして働く可能性があると考えられる。これらの結果から、扁桃体に比べ ACC の活動量を比較した効果量が小さいことから、否定性バイアスの影響は小さいことが示唆された。

【結論】 健常者に不快画像を提示すると、刺激条件にかかわらず扁桃体の活性化とACCの不活性化が観察された。しかし、快画像が提示されたST条件では、扁桃体の活性化と腹側ACCの不活性化は観察されなかった。これらの結果から、快画像を提示する短時間の単純な刺激パラダイムでは、扁桃体と腹側ACCに対する否定性バイアスの影響が顕著になる可能性が示唆された。扁桃体や背側・腹側ACCなどの解剖学的な神経領域の活動が否定性バイアスの影響を受け、それが刺激パラダイムの長さにも影響される。そのため、単純・複雑なパラダイムなどの視覚刺激パラダイムを設計する際には、課題の長さを適切に考慮する必要があると考えられる。

DH19103 吉田　宜清

目 次

Introduction

Major depressive disorder (MDD) is one of the most common mental health disorders worldwide [1]. Studies of functional magnetic resonance imaging (fMRI) have reported that MDD patients show dysfunction of the anterior cingulate cortex (ACC) and limbic system, especially the amygdala [2]. Recent fMRI studies have reported that amygdala and ACC dysfunction is a reproducible and good biomarker of MDD [3].

When using amygdala and ACC activation as biomarkers of MDD, a short and simple stimulation paradigm in MRI scan helps reduce the burden on patients. It is well known that the small spatial dimensions of the scanner tubes and the high noise level of the MRI machine elicit anxiety in patients [4] and that patients are instructed to reduce body movements to prevent artifacts during an MRI scan [5]. If the stimulation paradigm to activate the amygdala and ACC is short and simple, we can reduce the anxiety and body movements of patients during the MRI scan. However, when we employ a short and simple stimulation paradigm, we should consider how the paradigm would modulate the amygdala or ACC activation. One possible factor that we should care about is the negativity bias, which is the idea that negative (unpleasant) stimuli evoke a more pronounced response than equally extreme and arousing positive (pleasant) stimuli [6]. Furthermore, studies using electroencephalography have reported that negative stimuli are processed faster than positive stimuli [7]. Given the fact that negative stimuli elicit a stronger response and are processed faster than positive stimuli, amygdala activation by negative but not positive stimuli would be observed even in the short stimulation paradigm. Thus, there is a possibility that negativity bias would be observed when the short stimulation paradigm is employed, while it would be reduced if the stimulation paradigm is long enough to process positive stimuli.

To our best knowledge, no studies have investigated the relationship between the length of the stimulation paradigm and activation in the amygdala and ACC from the viewpoint of the negativity bias. Investigating the effect of negativity bias on amygdala activation in the short stimulation paradigm could be crucial because negativity bias could be a potential cognitive trait associated with vulnerability to depression [8]. In the present study, we aimed to assess the effects of negativity bias in the short and long emotional picture stimulation paradigms on the activation of emotion-related brain regions, including the amygdala and ACC. We employed two experimental conditions: (1) the short-simple condition, in which emotional pictures were presented for 130 seconds; and (2) the long-complex condition, in which pictures were presented for 300 seconds, similar to the paradigm used in treatment effect assessment [9]. We hypothesized that negativity bias could be observed in the short-simple condition, while negativity bias would be reduced in the long-complex condition.

Methods

Participants

Twenty-seven right-handed healthy volunteers (7 women and 20 men, average age of 22.4 ± 2.48 years, range = 20–30 years), with no history of current or past psychiatric disorders or substance abuse, participated in the experiment. The Research Ethics Committee of the Institute of Medical Science, University of Tokyo, approved the study protocols (29-51-A1120). Written informed consent was obtained from each participant before inclusion in the study.

Task and procedures

Forty pleasant pictures (P), 40 unpleasant pictures (U), and 15 neutral pictures (N) were selected from the

international affective picture system (IAPS) as visual stimuli for the emotional pictures viewing task [10]. For pleasant and unpleasant images, the same picture was not used in one task. The mean valence scores of the pleasant, unpleasant, and neutral pictures were 7.7, 3.0, and 5.3, respectively. The mean arousal scores were 5.0 for pleasant, 5.4 for unpleasant, and 3.2 for neutral pictures. The present study used two conditions. One was a short-simple task (ST) condition, and the other was a long-complex task (LT) condition. The number of visual stimuli and the length of time in the LT condition was larger and longer, respectively, than that in the ST condition. The ST condition consisted of five blocks of pictures, and the order of blocks was fixed (N–U–N–P–N). The number of pictures in one block was 10 with a two-second presentation time for each picture in the U and P blocks (20 seconds). The N block presented six pictures with a five-second presentation time (30 seconds). The total time taken for the ST condition was 130 seconds. The LT condition consisted of 10 blocks of pictures, and the order of blocks was counterbalanced between participants (pattern A: N–U–N–U–N–N–P–N–P–N or pattern B: N–P–N–P–N–N–U–N–U–N). The number of pictures in all blocks was 15, with a two-second presentation time for each picture (30 seconds). The total time taken for the LT condition was 300 seconds. Because of the longer duration of the LT condition, participants were asked to press a button with their right index finger each time the picture was changed to confirm they were awake. One scan session contained the ST and LT conditions, and the order of conditions was fixed as ST-LT (Fig. 1). The scan session was repeated two times. The presentation of visual stimuli was controlled using the E-Prime 2.0 software (Psychology Software Tools, Pittsburgh, PA), and the stimuli were back-projected to the center of a screen located near the scanner from a liquid-crystal-display video projector. Participants saw the stimuli through a movable mirror that was set on the head coil.

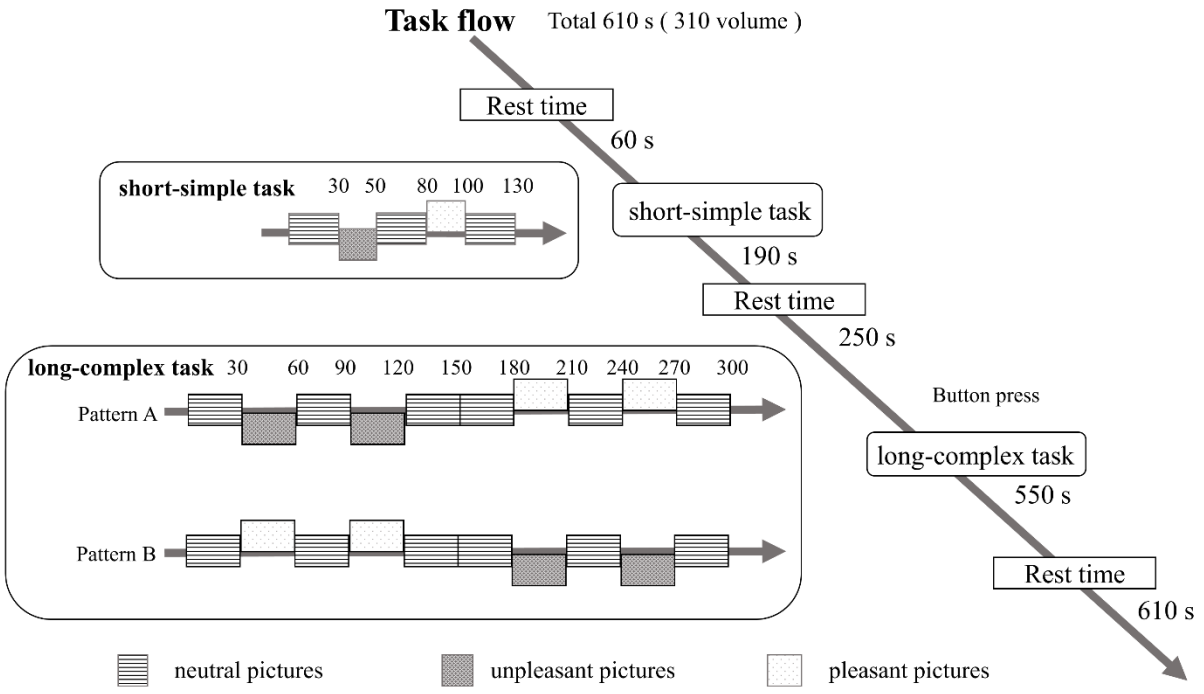

Fig. 1

Image acquisition

Whole-brain functional and anatomical images were acquired using a 3.0 Tesla clinical MRI scanner (MAGNETOM, Skyra, Siemens AG, Healthcare Sector, Erlangen, Germany) with Syngo MR E11 software and a 20-channel head matrix coil located at the Research Hospital, the Institute of Medical Science, the University of Tokyo. The participant's head was immobilized using head cushions and headphones within the scanner coil. T2*-weighted functional MRI data were acquired using a single-shot echo-planar (EPI) sequence (echo time [TE] = 30 ms, repetition time [TR] = 2.0 s, flip angle [FA] = 80°, slice thickness 4.0 mm, gap 1.0 mm, matrix 64 × 64, field of view [FOV] 240 mm, in-plane resolution 3.8 mm × 3.8 mm, 315 image volumes). The 35 transversal slices were tilted with a 30° reverse angulation (anterior upward) from the anterior commissure - posterior commissure line to minimize drop-out artifacts in the orbitofrontal and medial temporal regions [11]. The first three volumes of the EPI sequence were discarded to ensure a steady-state signal of the MRI. High-resolution anatomical images were acquired using a T1-weighted magnetization prepared rapid acquisition with gradient echo with 176 transverse slices (TE = 2.45 ms, TR = 2.2 s, inversion time = 900 ms, FA = 8°, slice thickness 1.0 mm, no gap, matrix 256 × 256, FOV 240 mm, in-plane resolution 0.9 mm × 0.9 mm) for coregistration of functional data.

Image analysis

Functional imaging data analysis was performed using the Statistical Parametric Mapping software (SPM12: Wellcome Department of Cognitive Neurology, London, UK; www.fil.ion.ucl.ac.uk/spm) implemented in MATLAB (R2017a: Mathworks, Natick, MA, USA). First, the EPI images were realigned to the first volume during preprocessing to correct for head movements using the unwarp option. Realignment parameters were checked to discern any potential participants with excessive head movement, which was defined as any displacement of more than one voxel (3.8 mm) from the position of the first acquired fMRI volume in a session. Second, the time series were corrected for differences in slice acquisition time with reference to the slice acquired in the middle of the acquisition time. Third, the EPI images were coregistered with the T1 anatomical images of each subject, and parameter files for spatial normalization into a standard template (Montreal Neurological Institute, MNI) were constructed for individual T1 anatomical images using a standard T1 template. All coregistered EPI volumes were spatially normalized into an approximate standard space, resliced to a resolution of 2-mm cubic voxels, and smoothed using a 6-mm full-width half at the maximum of the Gaussian filter kernel. The time series for each voxel was high-pass filtered using a 1/128 Hz cut-off to remove low-frequency noise and signal drift.

fMRI data were analyzed using a general linear model in SPM12. Effects of interest were modeled using six regressors: (1) unpleasant block in the ST, (2) neutral blocks in the ST, (3) pleasant block in the ST, (4) unpleasant blocks in the LT, (5) neutral blocks in the LT, and (6) pleasant blocks in the LT. All regressors were convolved using a canonical hemodynamic response function. Six motion parameters were also included as regressors of no interest. At the first analysis level, eight contrast images were constructed: (1) ST unpleasant > ST neutral, (2) ST pleasant > ST neutral (3) LT unpleasant > LT neutral, (4) LT pleasant > LT neutral, (5) ST neutral > ST unpleasant, (6) ST neutral > ST pleasant, (7) LT neutral > LT unpleasant, and (8) LT neutral > LT pleasant.

The first half of the eight contrast images were used to identify the brain regions activated with emotional picture viewing, and the second half was used to identify the deactivated brain regions. At the second level analysis, the single-subject maps were combined at the group level in a random-effects analysis to produce statistical parametric maps of group activation. One-sample *t*-tests were performed to investigate the activation of each of the

eight contrasts described above. The threshold for significance was set at $p < 0.01$, with false discovery rate (FDR) correction at peak level (cluster extent, k > 5). All local maxima are reported as MNI coordinates, and relevant anatomical landmarks were identified using the anatomical automatic labeling library (AAL3; https://www.gin.cnrs.fr/en/tools/aal/) and the atlas of the average MNI brain [12].

Regions of interest analysis

For regions of interest (ROI) analysis, we used the bilateral amygdala and ACC as anatomical ROIs (http://marsbar.sourceforge.net/download.htm), and beta values were extracted for each participant [13]. Beta values were measured for the following four blocks of regressors: (1) ST unpleasant block, (2) ST pleasant block, (3) LT unpleasant block, and (4) LT pleasant block. We conducted two separate ROI analyses. The first ROI analysis included both sessions. Four beta values were subjected to two paired *t*-tests (ST unpleasant vs. ST pleasant, and LT unpleasant vs. LT pleasant) for each brain region to estimate the effect of negativity bias in each stimulation paradigm. The Bonferroni correction was used considering multiple comparisons, and the α level was set at $p < .025$. The second ROI analysis was performed to estimate whether the effect of negativity bias would change between the sessions. Eight beta values (4 beta values × 2 sessions) were extracted from the two sessions separately. Four paired *t*-tests (ST unpleasant vs. ST pleasant in the first session, LT unpleasant vs. LT pleasant in the first session, ST unpleasant vs. ST pleasant in the second session, and LT unpleasant vs. LT pleasant in the second session) were performed to estimate the negativity bias in each session. The α level was set at $p < .0125$ for the second ROI analysis. Data on beta values were analyzed using the EZR statistical package [14]. We calculated the standardized effect size (Cohen's *d*) calculated by standardizing the difference between the mean values.

Results

Image analysis

Table 1 and Fig. 2 show the activated brain regions in contrast images in the ST and LT conditions for all sessions. For the unpleasant pictures, the contrast image of ST unpleasant > ST neutral showed significant activation in the bilateral amygdala in the ST condition. The LT unpleasant > LT neutral contrast image revealed significant activation in the bilateral amygdala that expanded to the bilateral hippocampus and right fusiform gyrus in the LT condition. For the pleasant pictures, a significant activation in the bilateral amygdala in the LT condition (LT pleasant > LT neutral) was observed. In contrast, no significant activation in the amygdala was observed in the ST condition (ST pleasant > ST neutral, see white arrows in Fig. 2).

Table 2 and Fig. 2 show the deactivation of brain regions during the presentation of unpleasant and pleasant pictures compared to the presentation of neutral pictures for the two sessions. The analysis showed ACC deactivation during the presentation of pleasant and unpleasant pictures, regardless of the stimulation paradigm. Although deactivation was found in the dorsal ACC (Table 2), the ventral ACC did not show deactivation only in the ST neutral pictures > ST pleasant contrast image (see yellow arrows in Fig. 2).

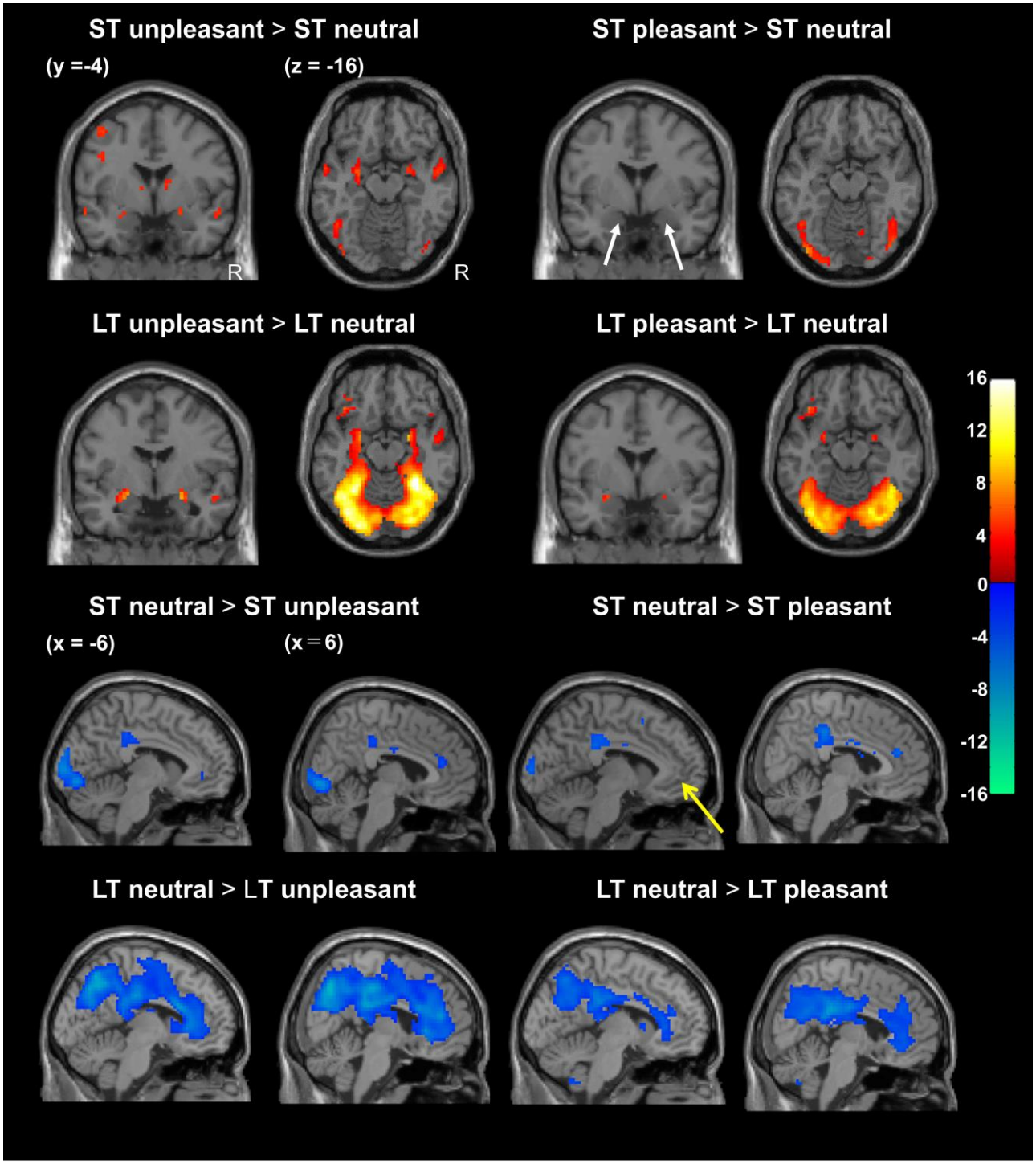
ST unpleasant > ST neutral
(y =-4)
(z = -16)
R
R
ST pleasant > ST neutral
LT unpleasant > LT neutral
LT pleasant > LT neutral
16
12
8
4
0
-4
-8
-12
-16
ST neutral > ST unpleasant
(x = -6)
(x = 6)
ST neutral > ST pleasant
LT neutral > LT unpleasant
LT neutral > LT pleasant

Fig. 2

Table 1. Results of Z-scores for the brain areas during the unpleasant or pleasant > neutral condition contrasts

task	Regions	MNI coordinates, mm			z-score	voxels
		x	*y*	*z*		
ST Unpleasant > ST Neutral	L Middle temporal gyrus	-51	-64	13	6.86	386
	R Superior / middle temporal gyrus	60	-55	7	6.18	201
	R, L Cerebellum crus2	-3	-76	-35	5.17	28
	L Precuneus / cuneus	-6	-64	16	4.86	351
	L Hippocampus / amygdala	-27	-16	-8	4.57	31
	L Thalamus	-3	-22	7	4.48	114
	R Cerebellum 7b, 8	15	-76	-44	4.37	20
	L Precentral gyrus	-42	-4	55	4.36	26
	L Medial superior frontal gyrus	-6	50	25	4.32	34
	R Superior temporal gyrus	54	-4	-11	4.31	14
	L Inferior occipital gyrus	-42	-85	-11	4.19	8
	R Posterior cingulate cortex	18	-46	4	4.1	7
	R Amygdala	24	-1	-14	3.97	6
	L Superior temporal gyrus	-57	-1	-14	3.94	7
	L Precentral gyrus	-45	2	34	3.91	9
LT Unpleasant > LT Neutral	R Fusiform gyrus/ R, L Amygdala	33	-67	-8	7.81	6,236
	L Pars orbitalis of inferior frontal gyrus	-42	26	-11	5.16	52
	L Medial superior frontal gyrus	-3	59	31	5.15	77
	L Precentral gyrus	-51	5	49	4.42	89
	L Superior / Inferior parieral lobule	-24	-64	52	4.39	46
	R Middle frontal gyrus	57	14	40	4.38	38
	L Cerebellum 9, 10	-15	-46	-44	4.35	6
	R Superior temporal gyrus	45	20	-20	4.16	12
	R Cerebellum 9	15	-43	-47	4.14	10
	R Superior parietal gyrus	27	-55	55	3.92	25
	R Superior / middle temporal gyrus	51	-4	-17	3.59	7
ST Pleasant > ST Neutral	L Middle temporal gyrus	-51	-67	10	5.93	489
	R Middle temporal gyrus	54	-58	13	5.5	304
	L Fusiform gyrus	-39	-85	-14	5.45	45
	R Calcarine cortex / lingual gyrus	9	-64	10	4.79	648
LT Pleasant > LT Neutral	R Calcarine sulcus/ occiptal gyrus	21	-94	-2	7.56	4,394
	L Parahippocampus gyrus / thalamus	-18	-31	-2	5.89	245
	L Posterior orbitofrontal cortex /	-39	26	-14	4.84	140

	pars orbitalis of inferior frontal gyrus					
	L Amygdala / putamen	-24	-1	-14	4.09	15
	L Cerebelum Crus2, 7b	-6	-76	-38	3.97	17
	L Medial superior frontal gyrus	-6	59	34	3.85	80
	L Thalamus	-6	-13	7	3.80	18
	R Amygdala	24	-4	-14	3.77	11
	R Precentral gyrus	54	11	40	3.45	68

R: right hemisphere, L: left hemisphere, ACC; Anterior cingulate cortex ST: short-simple task condition, LT: long-complex task condition, MNI: Montreal Neurological Institute. $p < 0.01$ (FDR correction) k > 5

Table 2. Results of Z-score for brain areas during neutral > unpleasant or pleasant condition contrasts

task	Regions	MNI coordinates, mm			z-score	voxels
		x	*y*	*z*		
ST neutral	R Fusiform gyrus / parahippocampal gyrus	30	-43	-14	7.69	3,404
> ST	L Superor parietal loube	-18	-67	40	5.13	224
unpleasant	L Middle frontal gyrus /	-33	23	58	4.75	61
	L Superior Frontal gyrus					
	R ACC	12	38	16	4.6	41
	L Posterior cingulate cortex	-6	-34	40	4.32	83
	R Caudate nucleus / putamen	15	23	4	4.02	16
	R Cerebellum crus2, crus1	39	-64	-41	3.9	34
	R Superior frontal gyrus	30	29	58	3.84	83
	R Middle frontal gyrus	39	35	19	3.81	27
	R Middle cingulate cortex	6	-10	31	3.79	8
	L ACC	-9	41	-2	3.75	27
	R Pars triangularis of inferior frontal gyrus	39	41	-2	3.63	26
	L Supramarginal gyrus	-54	-40	52	3.61	10
LT neutral	L Superior Frontal gyrus	-30	32	34	7.3	26,842
> LT	L Cerebelum crus2, crus1	-39	-64	-41	6.29	552
unpleasant	R Cerebelum crus1, 6	36	-61	-38	3.85	237
	L Cerebelum 8	-12	-64	-50	3.47	10
ST neutral	R Fusiform gyrus / parahippocampal gyrus	30	-43	-14	7.54	204
> ST	L Fusiform gyrus / lingual gyrus	-27	-49	-14	6.25	325
pleasant	L Superior / middle Occipital gyrus	-12	-94	19	5.51	160
	R Superior / middle occipital gyrus	27	-82	16	5.47	79
	R ACC	9	38	16	5.35	42

	R Posterior cingulate cortex	6	-31	40	5.19	176
	L Middle cingulate cortex / caudate nucleus	-12	-10	28	4.76	33
	R Putamen / insula	24	20	-5	4.63	15
	L Angular gyrus / Supramarginal gyrus	-42	-46	34	4.54	59
	R Pars orbitalis / pars triangularis of inferiror frontal gyrus	39	38	-5	4.51	50
	R Inferior parietal lobule / Supramarginal gyrus	42	-40	43	4.51	157
	L Insula / amygdala	-33	-1	-17	4.31	12
	L Supplementary motor cortex	-9	11	52	4.17	12
	R Pars opercularis / pars triangularis of inferior frontal gyrus	45	14	13	4.16	21
	R Middle occipital gyrus	36	-76	40	4.16	8
	R Thalamus / caudate nucleus	12	-7	25	4.13	34
	R Superior / middle frontal gyrus	24	14	55	3.94	50
	R Middle frontal gyrus / pars triangularis of inferior frontal gyrus	42	35	22	3.91	14
	L Middle frontal gyrus	-39	23	52	3.9	11
	R Superior frontal gyrus	18	8	64	3.86	6
	R Middle temporal gyrus	66	-22	-11	3.8	20
	R Supramarginal gyrus	60	-34	25	3.79	6
	R Middle temporal gyrus	51	-40	-8	3.77	6
	L Middle temporal gyrus	-60	-43	-5	3.73	9
	L Superior pariental lobule	-18	-67	40	3.7	10
	R Middle frontal gyrus	30	29	31	3.69	11
	L Middle frontal gyrus	-39	35	22	3.62	6
	R Anterior / middle cingulate cortex	9	17	22	3.6	9
LT neutral > LT pleasant	R, L Posterior cingulate cortex/ R, L ACC	6	-34	28	6.14	10,343
	L Cerebelum posterior lobe	-39	-67	-47	5.1	305
	R Cerebelum anterior lobe	18	-61	-26	4.92	191
	R Pars opercularis of inferiror frontal gyrus	54	8	16	4.68	96
	R Cerebelum posterior lobe	15	-64	-50	4.01	22
	L Cerebelum posterior lobe	-6	-58	-50	3.66	19
	L Superior/ middle frontal gyrus	-21	53	7	3.2	8
	R Precuneus	30	-55	19	3.02	7

R: right hemisphere, L: left hemisphere, ACC; Anterior cingulate cortex ST: short-simple task condition, LT: long-complex task condition, MNI: Montreal Neurological Institute. $p < 0.01$ (FDR correction) $k > 5$

Table 3. Results of beta values for the amygdala and ACC in each and all sessions

session	contrast	Amygdala				ACC			
		short-simple		long-complex		short-simple		long-complex	
1st	u	0.177 ± 0.149	*	0.163 ± 0.332	n.s.	-0.0333 ± 0.190	n.s.	-0.252 ± 0.376	*
	p	0.0779 ± 0.163	d=0.63	0.0800 ± 0.385		-0.0730 ± 0.144		-0.150 ± 0.344	d=0.28
2nd	u	0.0897 ± 0.141	*	0.0641 ± 0.293	n.s.	-0.0965 ± 0.201	n.s.	-0.301 ± 0.314	n.s.
	p	-0.0130 ± 0.138	d=0.74	0.00719 ± 0.303		-0.0756 ± 0.203		-0.218 ± 0.358	
combined	u	0.267 ± 0.208	*	0.2269 ± 0.495	*	-0.130 ± 0.271	n.s.	-0.554 ± 0.495	*
	p	0.0645 ± 0.205	d=0.98	0.0874 ± 0.502	d=0.28	-0.149 ± 0.251		-0.369 ± 0.516	d=0.37

The anatomical position sets the regions of interest in MarsBar and shows the extracted and shows the mean and standard deviation of the extracted beta values. Statistical analysis was performed using a paired *t*-test. A Bonferroni correction was used to compare multiplicity. Therefore, the significance level was set at $p < 0.025$ for all sessions and $p < 0.0125$ for each session. The effect size (d) was calculated by standardizing the difference between the mean values. u; unpleasant pictures p; pleasant pictures, *; significantly different, and n.s.; no significant difference.

Regions of interest analysis

Table 3 shows the results of ROI analyses for both the analysis of all the sessions combined and for the analysis where the data of each session was analyzed separately. The difference in the beta values for the amygdala between unpleasant and pleasant pictures combining all sessions was significant between the ST condition ($t(26) = 2.46$, $p < 0.025$) and the LT condition ($t(26) = 6.87$, $p < 0.025$). The effect size of the ST condition was 0.98, while that of the LT condition was 0.28. The beta values for the ACC on combining all sessions were not significantly different between pleasant and unpleasant pictures in the ST condition ($t(26) = 0.382$), whereas there was a significant difference in the LT condition between the values for pleasant and unpleasant pictures ($t(26) = -2.84$, $p < 0.025$). The effect size of the LT condition was 0.37.

We examined the difference in beta values between pleasant and unpleasant pictures for each session in the amygdala and ACC. The first session of the ST condition showed a significant difference between pleasant and unpleasant pictures ($t(26) = -3.44$, $p < 0.0125$), whereas the LT condition showed no significant difference ($t(26) = -2.25$). The beta values for the amygdala in the second session were significantly different between emotional pictures (pleasant vs. unpleasant) in the ST condition ($t(26) = -4.99$, $p < 0.0125$). On the other hand, there was no significant difference between the emotional pictures in the LT condition ($t(26) = -1.32$) in the second session. Beta values of ACC showed no significant difference between the emotional pictures in the first and second sessions of ST condition (ST in the first session: $t(26) = -1.32$; ST in the second session: $t(26) = -0.666$). In the LT condition, there was a significant difference between the emotional pictures in the first session ($t(26) = 2.87$, $p < 0.0125$), and no significant difference in the second session ($t(26) = -1.44$). The effect size of the LT condition in the first session, where we

found a significant difference, was 0.28.

Discussion

The contrast image analyses in the present study showed that the amygdala was activated both in the ST and LT condition when unpleasant pictures were presented. For pleasant picture presentation, the contrast image analyses in the ST condition did not show any significant activation in the amygdala (see white arrows in Fig. 2). The extracted amygdala beta values for pleasant pictures were significantly smaller than the values for unpleasant pictures in the first, second, and combined sessions for the ST condition, and the beta values for pleasant pictures in the ST condition were close to zero (Table. 3). In the LT condition, only the combined session showed that the amygdala beta value for pleasant picture presentation was significantly smaller than the value for the unpleasant picture presentation. Deactivation of the ACC was observed in both the ST and LT conditions with pleasant and unpleasant pictures. The extracted ACC beta values were significantly different between pleasant and unpleasant images in the first and combined sessions of the LT condition, while no difference was observed in the first, second, and combined sessions of the ST condition.

We discuss the effects of negativity bias on activity in the amygdala and ACC in the following sections.

Amygdala

The results the present study indicated that only the unpleasant, but not the pleasant pictures, could activate the amygdala even in the short and simple stimulation paradigm. As mentioned in the methods section, we ensured that the relative emotional valence and arousal score of the selected unpleasant pictures was relatively similar to that of the pleasant pictures. Therefore, we can exclude the possibility that the observed activation difference in the amygdala stems from the difference in the relative emotional valence and arousal score of the emotional pictures.

A possible explanation of the difference observed in the activation of the amygdala in response to pleasant and unpleasant pictures is the negativity bias. According to the theory of negativity bias, negative stimuli are processed faster and more efficiently than positive stimuli [7]. In the ST condition, the unpleasant pictures could be processed faster than the pleasant pictures, and this might be a reason for the difference observed in the activation of the amygdala for pleasant and unpleasant pictures in the ST condition.

The results of the ROI analysis in the ST condition also indicated that the extracted beta values for the amygdala in the first, second, and the combined sessions were significantly larger for unpleasant pictures than those for pleasant pictures. In particular, the effect sizes (*d*) were relatively large, and the maximum value (0.98) was observed in the combined sessions. These results suggest that the ST condition is affected by negativity bias from the first session to the second session. These results of the ROI analyses support the notion that the unpleasant pictures could be processed faster than the pleasant pictures, and this might be a reason for the larger activation of the amygdala for unpleasant pictures than that for pleasant pictures in the short and simple stimulation paradigm.

On the other hand, the results of the ROI analysis in the LT condition showed no difference in amygdala activity between pleasant and unpleasant pictures in the first and second sessions. Although the beta value in the combined sessions revealed a significant difference in amygdala activity between emotional pictures, the effect size (0.28) was smaller than that in the ST condition (0.98). These results indicate that the effect of negativity bias is reduced in the LT condition. If the effect of unpleasant pictures on the activity in the amygdala is cumulative, the effect of negativity bias should be the same or even greater as more emotional pictures are presented and repeated.

One possible reason for the reduced effect of negativity bias in the LT condition is the inhibition or habituation to repeatedly presented unpleasant pictures. Previous studies have shown that the amygdala rapidly habituates to repeatedly presented emotional visual stimuli [15], and the activity of the amygdala decreases as it habituates [16]. Therefore, we assume that the amygdala could habituate to unpleasant pictures in the LT condition because the region responded faster to unpleasant pictures than pleasant pictures. On the other hand, the effect of habituation to pleasant pictures might be small because amygdala activation to pleasant pictures was smaller than that to unpleasant pictures due to the slower processing of pleasant pictures. As a result, the effect of negativity bias in the LT condition would be reduced compared with that in the ST condition because of the differences in activity and habituation of the amygdala for pleasant and unpleasant pictures.

As we hypothesized, the effect of negativity bias on amygdala activation was more prominent in the short and simple conditions than that in the long and complex conditions. The findings of the present study suggest that the effect of negativity bias varies with the task condition of the visual stimulus. In particular, when employing a short and simple paradigm for pleasant stimuli, the effect of negativity bias is prominent, suggesting that setting an appropriate stimulation paradigm is crucial.

ACC

In the present study, contrast-image analyses showed the deactivation of the ACC in the ST and LT conditions for pleasant and unpleasant pictures. Similar to the results of the present study, there are reports that presentation of pictures from the IAPS deactivated the ACC [8]. However, other studies using emotional visual stimuli have reported both the activation and deactivation of the ACC [18]. These contradicting reports may be attributed to the differences in the subregions of the ACC. The ACC can be divided into the dorsal and ventral ACC. The dorsal ACC functions to identify the relevance of the incoming stimuli to guide the generation of appropriate behavior in response [18] and performs a regulatory role in the generation of emotions [19]. On the other hand, the ventral ACC, which has a strong connectivity to the amygdala [20], is thought to play an important role in emotional processing [17]. Some studies have reported that the activity of the ventral ACC negatively correlated with that of the amygdala. These facts suggest that the ventral ACC works as a mediator of the amygdala activity [21-23]. Moreover, the ventral ACC is strongly influenced by the negativity bias and its effect may represent a potential cognitive characteristic of depression in healthy individuals [20]. These reports indicate the importance of the examination of the effects of negativity bias on the ACC, which contributes to emotional processing. In the present study, pleasant pictures significantly deactivated the dorsal ACC in the ST conditions, whereas they neither activated nor deactivated the ventral ACC. The results of the dorsal ACC indicate that the region is less affected by negativity bias because the deactivation in response to pleasant pictures in the ST condition indicates that the dorsal ACC processed faster, even in the case of pleasant pictures. On the other hand, the ventral ACC was deactivated only for unpleasant pictures in the ST condition, suggesting that the ventral ACC is affected by negativity bias. Therefore, results support the idea that the ventral ACC is sensitive to negativity bias and the region functions as a controller of emotional processing [17,20].

In the results of the ROI analysis on the ACC that included both the dorsal and ventral ACC, there was no difference in the beta values between pleasant and unpleasant pictures in the ST condition. These results indicate that the effect of the negativity bias on the ACC was small, and the effect was different for the amygdala and ACC. In case of the results of the ROI analysis in the LT condition, there was a significant difference between pleasant and

unpleasant pictures in the first and combined sessions, whereas there was no difference in the second session. We assume that the ACC inhibited the amygdala during the presentation of unpleasant pictures in the first session. In the second session, the ACC reduced the inhibition of the amygdala because the amygdala was habituated and reduced its activity in response to unpleasant pictures. As a result, there was no difference in the deactivation of the ACC between pleasant and unpleasant pictures in the second session. In the ROI analysis in the combined sessions, there was a significant difference between pleasant and unpleasant pictures. However, the effect sizes of ACC deactivation in the LT condition in the first session and the combined sessions were small between pleasant and unpleasant pictures. Thus, we suggest that the effect of negativity bias on the ACC could be small in a long and complex stimulation paradigm.

In summary, the ACC, which included both the dorsal and ventral ACC, in the short and simple task showed no significant difference in deactivation in response to emotional pictures. In the long and complex task condition, we showed significant differences in response to emotional pictures; however, the effect sizes were small, suggesting that the effect of negativity bias was also small.

Conclusion

In conclusion, we observed amygdala activation and ACC deactivation in the simple and short task condition when healthy participants were presented with visual IAPS stimuli with unpleasant pictures. The amygdala activation and the ventral ACC deactivation were not observed in the ST condition for the presentation of the pleasant pictures. These results suggest that the effect of negativity bias on the amygdala and the ventral ACC could be pronounced in the short and simple stimulation paradigm of pleasant pictures. On the other hand, the ACC, which includes ventral and dorsal ACC, was affected by negativity bias only in the long and complex task conditions. Therefore, the task length should be given appropriate consideration while designing visual stimulus paradigms, such as simple or complex paradigm, because the effect of negativity bias depends on the activity of the anatomical neural regions and their subregions, including the amygdala and dorsal and ventral ACC, which is in turn influenced by the length of the task.

Acknowledgments

The authors thank the members of the Department of Radiology, Research Hospital, the Institute of Medical Science the University of Tokyo.

Conflicts of interest

The authors declare that they have no conflicts of interest.

References

1. Wang L, Hermens DF, Hickie IB, Lagopoulos J. A systematic review of resting-state functional-MRI studies in major depression. *J. Affect. Disord.* 2012; 142 (1–3): 6–12.

2. Chana G, Landau S, Beasley C, Everall IP, Cotter D. Two-dimensional assessment of cytoarchitecture in the anterior cingulate cortex in major depressive disorder, bipolar disorder, and schizophrenia: Evidence for decreased neuronal somal size and increased neuronal density. *Biol. Psychiatry* 2003; 53 (12): 1086–1098.

3. Arnone D. Functional MRI findings, pharmacological treatment in major depression and clinical response.

Prog. Neuro-Psychopharmacology Biol. Psychiatry 2019; 91 (August 2018): 28–37.

4. Grey SJ, Price G, Mathews A. Reduction of anxiety during MR imaging: A controlled trial. *Magn. Reson. Imaging* 2000; 18 (3): 351–355.

5. Godenschweger F, Kägebein U, Stucht D, Yarach U, Sciarra A, Yakupov R, et al. Motion correction in MRI of the brain. *Phys. Med. Biol.* 2016; 61 (5): R32–R56.

6. Gollan JK, Connolly M, Buchanan A, Hoxha D, Rosebrock L, Cacioppo J, et al. Neural substrates of negativity bias in women with and without major depression. *Biol. Psychol.* 2015; 109: 184–191.

7. Kuhbandner C, Spachtholz P, Pastötter B. Bad things come easier to the mind but harder to the body: Evidence from brain oscillations. *Cogn. Affect. Behav. Neurosci.* 2016; 16 (4): 768–778.

8. Dai Q, Wei J, Shu X, Feng Z. Negativity bias for sad faces in depression: An event-related potential study. *Clin. Neurophysiol.* 2016; 127 (12): 3552–3560.

9. Chen YT, Huang MW, Hung IC, Lane HY, Hou CJ. Right and left amygdalae activation in patients with major depression receiving antidepressant treatment, as revealed by fMRI. *Behav. Brain Funct.* 2014; 10 (1): 1–11.

10. Lang Bradley, M.M., & Cuthbert, B.N. PJ. International affective picture system (IAPS): Affective ratings of pictures and instruction manual. 2008.

11. Deichmann R, Gottfried JA, Hutton C, Turner R. Optimized EPI for fMRI studies of the orbitofrontal cortex. *Neuroimage* 2003; 19 (2): 430–441.

12. Petrides, M. Atlas of the Morphology of the Human Cerebral Cortex on the Average MNI Brain. Academic Press, New York, 2019

13. Brett M, Anton JL, Valabregue R, Poline JB. Region of interest analysis using an SPM toolbox. *Neuroimage* 2002; 16: 497.

14. Kanda Y. Investigation of the freely available easy-to-use software "EZR" for medical statistics. *Bone Marrow Transplant.* 2013; 48 (3): 452–458.

15. Breiter HC, Etcoff NL, Whalen PJ, Kennedy WA, Rauch SL, Hyman SE, et al. Response and Habituation of the Human Amygdala during Visual Processing of Facial Expression bilateral amygdala lesions have demonstrated impair-ments in recognition of fear (Adolphs et al finds support from aversive (fear) conditioning experi-*Nuclear Ma. *Neuron* 1996; 17: 875–887.

16. Zald DH. The human amygdala and the emotional evaluation of sensory stimuli. *Brain Res. Rev.* 2003; 41 (1): 88–123.

17. Bush G, Luu P, Posner MI. Cognitive and emotional influences in anterior cingulate cortex. *Trends Cogn. Sci.* 2000; 4 (6): 215–222.

18. Seeley WW, Menon V, Schatzberg AF, Keller J, Glover GH, Kenna H, et al. Dissociable intrinsic connectivity networks for salience processing and executive control. *J. Neurosci.* 2007; 27 (9): 2349–2356.

19. Etkin A, Egner T, Kalisch R. Emotional processing in anterior cingulate and medial prefrontal cortex. *Trends Cogn. Sci.* 2011; 15 (2): 85–93.

20. Stevens FL, Hurley RA, Taber KH. Anterior cingulate cortex: Unique role in cognition and emotion. *J. Neuropsychiatry Clin. Neurosci.* 2011; 23 (2): 121–125.

21. Hadas I, Sun Y, Lioumis P, Zomorrodi R, Jones B, Voineskos D, et al. Association of Repetitive Transcranial Magnetic Stimulation Treatment With Subgenual Cingulate Hyperactivity in Patients With Major Depressive Disorder: A Secondary Analysis of a Randomized Clinical Trial. *JAMA Netw. open* 2019; 2 (6): e195578.

22. Johnstone T, Van Reekum CM, Urry HL, Kalin NH, Davidson RJ. Failure to regulate: Counterproductive recruitment of top-down prefrontal-subcortical circuitry in major depression. *J. Neurosci.* 2007; 27 (33): 8877–8884.
23. Urry HL, Van Reekum CM, Johnstone T, Kalin NH, Thurow ME, Schaefer HS, et al. Amygdala and ventromedial prefrontal cortex are inversely coupled during regulation of negative affect and predict the diurnal pattern of cortisol secretion among older adults. *J. Neurosci.* 2006; 26 (16): 4415–4425.

Legends for illustrations

Fig. 1 Schematic representation of the experimental paradigm.
For the session of 610 seconds, a set of pleasant, unpleasant, and neutral pictures from the international affective picture system database were presented within the two tasks: short-simple task and long-complex task. The short-simple task was divided into five blocks, each of which included the presentation of neutral, pleasant, and unpleasant pictures. The long-complex task was divided into 10 blocks. The order of the presentation of pleasant and unpleasant pictures in the long-complex task was counterbalanced between participants (Pattern A and Pattern B).

Fig. 2 Statistical parametric maps of the brain regions showed significant increases in the blood oxygenation level dependent image contrast associated with short-simple and long-complex task conditions ($p < 0.01$, false discovery rate corrected). White arrows indicate the amygdala, and yellow arrows indicate the ventral ACC. ST: short-simple task condition, LT: long-complex task condition, and R: right.

研究業績リスト

論文

1. Ohgami Y, Kotani Y, Yoshida N, et al. Voice, rhythm, and beep stimuli differently affect the right hemisphere preponderance and components of stimulus-preceding negativity. Biol Psychol. 2021;160(February):108048.
2. Yoshida N, Kotani Y, Ohgami Y, et al. Effects of negativity bias on amygdala and anterior cingulate cortex activity in short and long emotional stimulation paradigms. Neuroreport. 2021;32(6):531‐539.
3. Kotani Y, Ohgami Y, Yoshida N, et al. Anticipation process of the human brain measured by stimulus-preceding negativity (SPN). J Phys Fit Sport Med. 2017;6(1):7‐14.

学会発表

1. Ohgami Y, Kotani Y, Yoshida N, et al.: Information Flow of the Right Anterior Insula Revealed by fMRI-Constrained EEG Source Analysis. 2020 Virtual Annual Meeting of Society for Psychophysiological Research, Virtual, Oct. 2020.
2. Kotani Y, Yoshida N, Ohgami Y, et al.: The Effect of Task Length on Functional Connectivity of the Amygdala in a Picture Viewing Task. 2020 Virtual Annual Meeting of Society for Psychophysiological Research, Virtual, Oct. 2020.
3. Ohgami Y, Kotani Y, Yoshida N, et al.: Connectivity Dynamics of the Right Anterior Insula Revealed by EEG Source Analysis. Annual Meeting of the Organization of Human Brain mapping, Abstract Listings, p. 144, June 2020.
4. Kotani Y, Yoshida N, Ohgami Y, et al.: Functional Connectivity of Amygdala in a Simple and Short Picture Viewing Task. Annual Meeting of the Organization of Human Brain Mapping, Abstract Listings, p. 144, June 2020.
5. Ohgami Y, Kotani Y, Yoshida N, et al.: Connectivity dynamics between the right anterior insula and the anterior cingulate cortex during anticipation of interoceptive response. The 59th Annual Meeting of Society for Psychophysiological Research, Washington, S40, Sept. 2019.
6. Kotani Y, Ohgami Y, Yoshida N, et al.: Activation in the amygdala in a simple and short picture viewing task for clinical application. The 59th Annual Meeting of Society for Psychophysiological Research, Washington, Sept. 2019.
7. Kotani Y, Ohgami Y, Yoshida N, et al.: Activation in the amygdala in a simple and short picture viewing task. Annual Meeting of the Organization of Human Brain Mapping, Rome, June 2019.
8. Ohgami Y, Kotani Y, Yoshida N, et al.: Connectivity dynamics between the right anterior insula and the anterior cingulate cortex. Annual Meeting of the Organization of Human Brain Mapping, Rome, June 2019.
9. Ohgami Y, Kotani Y, Yoshida N, et al.: Neural substrates of early and late SPN before face, word and symbol stimuli, The 58th Annual Meeting of Society for Psychophysiological Research, Quebec, Oct. 2018.
10. Kotani Y, Ohgami Y, Yoshida N, et al.: Different roles of left and right anterior insula in anticipation of behavioral information and reward information, The 58th Annual Meeting of Society for Psychophysiological Research, Quebec, Oct. 2018.
11. Kotani Y, Ohgami Y, Yoshida N, et al.: fMRI constrained source analysis on stimulus-preceding negativity before face, word and symbol. Annual Meeting of the Organization of Human Brain Mapping, Singapore, June 2018.
12. Ohgami Y, Kotani Y, Yoshida N, et al.: Functional dissociation of left and right anterior insula in anticipation, Annual Meeting of the Organization of Human Brain Mapping, Singapore, June 2018.

13. Ohgami Y, Kotani Y, Yoshida N, et al.: The contents of auditory stimulus affect brain regions involved in anticipation: An fMRI study. The 57th Annual Meeting of Society for Psychophysiological Research, Vienna, Oct. 2017.
14. Kotani Y, Ohgami Y, Yoshida N, et al.: Components of Stimulus-preceding negativity prior to voice, beep, and rhythmic sound. The 57th Annual Meeting of Society for Psychophysiological Research, Vienna, S75, Oct. 2017.
15. Kotani Y, Ohgami Y, Yoshida N, et al.: Hemispheric difference in anticipation process of voice, beep, and rhythmic sound. Annual Meeting of the Organization of Human Brain Mapping, Vancouver, June 2017.
16. Ohgami Y, Kotani Y, Yoshida N, et al.: Anticipation process for voice is faster than anticipation process for rhythmic sound. Annual Meeting of the Organization of Human Brain Mapping, Vancouver, June 2017.
17. Ohgami Y, Kotani Y, Yoshida N, et al.: Stimulus-preceding negativity prior to voice, beep, and rhythmic sound. The 56th Annual Meeting of Society for Psychophysiological Research, Seattle, Sept. 2016.
18. Kotani Y, Ohgami Y, Yoshida N, et al.: Activation in the right anterior insular cortex in anticipation of reward information. The 56th Annual Meeting of Society for Psychophysiological Research, Seattle, Sept. 2016.
19. 大上 淑美, 小谷 泰則, 吉田 宜清, ―ら.: 音声刺激の予期は刺激先行陰性電位(SPN)の前期成分を賦活させる. 第38回日本生理心理学会大会, 広島, 2020.8.
20. 大上 淑美, 小谷 泰則, 吉田 宜清, ―ら.: 右前部島皮質と前部帯状皮質における結合性の時間変化. 第37回日本生理心理学会大会, 越谷, 2019.3.
21. 小谷 泰則, 大上 淑美, 吉田 宜清, ―ら.: 単純な視覚刺激呈示課題における扁桃体の賦活. 第37回日本生理心理学会大会, 越谷, 2019.3.
22. 大上 淑美, 小谷 泰則, 吉田 宜清, ―ら.: fMRI制限ソース分析によるSPN前期成分と後期成分の発生源の同定. 第36回日本生理心理学会大会, 小倉, 2018.3.
23. 小谷 泰則, 大上 淑美, 吉田 宜清, ―ら.: 顕著性および行動適応に関する前部島皮質の機能的左右差. 第36回日本生理心理学会大会, 小倉, 2018.3.
24. 大上 淑美, 小谷 泰則, 吉田 宜清, ―ら.: 聴覚刺激による刺激先行陰性電位（SPN）の前期成分と後期成分, 第35回日本生理心理学会大会, 流山, 2017.8.
25. 吉田 宜清, 桐生 茂, 三木 聡一郎, ―ら.: 放射線画像研究会のための参加型会議システムの検討. 第73回日本放射線技術学会総会学術大会,横浜 2017.4.
26. 大上 淑美, 小谷 泰則, 吉田 宜清, ―ら.: 音声・メロディ音・ビープ音の予期と関連する刺激先行陰性電位 第34回日本生理心理学会大会, 名古屋, 2016.8.
27. 吉田 宜清, 桐生 茂, 赤井 宏行, ―ら.: CT灌流画像の基礎的評価に適したファントムの製作および検討. 第72回日本放射線技術学会総会学術大会, 横浜, 2016.4.
28. 小野口 昌久、 高山 輝彦、 川井 恵一、―ら.: パーキンソン病における心筋131I-MIBG集積低下の解明-マウスによる検証 第25回日本核医学技術学会総会学術大会, 仙台, 2005.6.
29. 畑山 郁美, 小野口 昌久, 高山 輝彦, ―ら.: 6-OHDA誘発パーキンソン病モデルラットにおける131I-MIBGの体内動態. 第24回日本核医学技術学会総会学術大会, 千葉, 2004.6.